Nonlinear Optical Technique for Precise Retardation Measurements

Stefano Cattaneo,[1,*] Oliver Zehnder,[2] Peter Günter,[2] and Martti Kauranen[1]

[1]*Optics Laboratory, Institute of Physics, Tampere University of Technology, P.O. Box 692, FIN-33101 Tampere, Finland*

[2]*Nonlinear Optics Laboratory, Institute of Quantum Electronics, Swiss Federal Institute of Technology, ETH Hönggerberg, CH-8093 Zürich, Switzerland*

(Received 18 December 2001; published 30 May 2002)

We present a highly sensitive nonlinear optical technique to measure optical retardation. The technique is based on second-harmonic generation from thin films using two beams at the fundamental frequency. The sensitive polarization dependence of the process allows measuring optical retardation very precisely. The technique relies on fundamental symmetry principles and does therefore not require complicated experimental arrangement or data analysis. The technique was demonstrated by determining the retardation of a nominal half-wave plate to a precision and repeatability better than $\lambda/10^4$.

DOI: 10.1103/PhysRevLett.88.243901 PACS numbers: 42.65.Ky, 42.25.Ja, 42.25.Lc

Polarization is a very fundamental property of light, necessary to account for the vectorial character of electromagnetic waves. Many processes in optics depend on the polarization states of the beams involved [1]. In addition, polarization mode dispersion seems to be the ultimate factor limiting the maximum data transmission rate in modern optical fibers [2]. Besides optics, the study of polarization is important in many other fields, such as astronomy, chemistry, biology, and remote sensing.

Certain optical quantities can be determined very accurately. The frequency of light, for instance, can soon be measured to a few parts in 10^{16} [3]. On the other hand, it is very difficult to measure precisely the polarization state of light. The most general polarization state is represented by elliptical polarization. The shape (ellipticity), the orientation (azimuth), and the handedness of the polarization ellipse can be determined if the relative amplitudes of two arbitrary orthogonal polarization components and their phase difference (retardation) are known, and vice versa [4]. Existing ellipsometric techniques allow determining the azimuth of the polarization ellipse to a precision of 10^{-6} rad [5]. The retardation induced by active components on a light beam can be measured to a precision on the order of $\lambda/10^8$ using, for example, an intracavity polarimeter [6] or optical heterodyne techniques [7]. A similar precision in retardation measurements of passive components, however, has been reached only for very particular cases, e.g., for supermirrors with ultralow birefringence [8]. It is therefore still a challenge to measure the retardation of common birefringent elements or the ellipticity of an arbitrary beam to a high degree of accuracy.

The difficulties in accurate retardation measurements are evident, for example, in the characterization of common wave plates, which are key components in applications where control and analysis of the polarization state of light are required. The most precise ellipsometric techniques used nowadays in the industry allow measuring the retardation of wave plates only to $\lambda/1000$ [9]. Alternative measurement techniques have reached a maximum precision of $\lambda/7000$ [10–13], but at the expense of complicated experimental setups and data analysis. A recent technique based on polarization modulation quotes a sensitivity on the order of $\lambda/10^5$ for small values of retardation [14,15]. A common feature of these and other techniques is that they require a careful alignment of several polarization components. This often leads to hampering factors such as varying retardation offsets that considerably lower the precision and repeatability of the techniques. It is therefore evident that any real advances in retardation measurements must be based on novel physical principles rather than improved instrumentation and data analysis.

We present a completely new technique for retardation measurements that has the potential of being superior to existing techniques in several important aspects. The technique is based on second-harmonic generation from thin films using two input beams at the fundamental frequency. The technique relies on fundamental symmetry properties of the nonlinear interactions and does not require sophisticated experimental arrangement or data analysis to achieve a high precision. In our initial demonstration of the technique using a relatively simple setup, we have already achieved a precision of $\lambda/10^4$. In addition, the technique does not rely on extremely careful alignment of the optical elements or of the beams involved.

We consider the geometry of Fig. 1. Two beams at the fundamental frequency ω and on the same plane of incidence are applied on a poled thin film with in-plane isotropy. The polarization state of the target beam (wave vector $\mathbf{k}_1$) is to be determined. To measure the phase shift (retardation) between two orthogonal components of the target polarization vector, a probe beam (wave vector $\mathbf{k}_2$) with a controllable polarization is used. Since we are interested in processes to which both the target and the probe beams contribute, coherent second-harmonic light is detected in the approximate direction $\mathbf{k}_1 + \mathbf{k}_2$ [16].

An arbitrary elliptical target polarization can be described as a sum of linear and circular polarization components. The circular component is known to break the symmetry of the setup and to result in a different response of second-harmonic generation to left- and right-hand

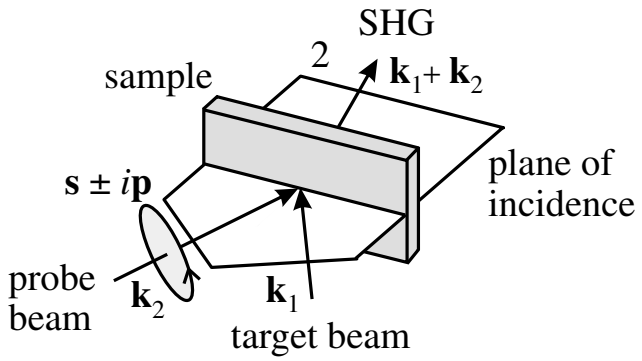

FIG. 1. Geometry of nonlinear retardation measurements. Two beams (target and probe) at the fundamental frequency ω and on the same plan of incidence intersect in a poled thin film. The intensity of the produced second-harmonic signal is measured.

circularly polarized probe beams [17]. This effect can be quantified by the normalized circular-difference response in the second-harmonic signal intensity,

$$\frac{\Delta I}{I} = \frac{I_{\text{left}} - I_{\text{right}}}{(I_{\text{left}} + I_{\text{right}})/2}, \tag{1}$$

where the subscripts refer to circular probe polarizations. This difference effect can be interpreted in terms of optical activity arising from the broken reflection symmetry of the experiment due to the circular target polarization. From another point of view, the effect arises from interference between the real and the imaginary parts of the vector describing the polarization state of the target beam [17]. The circular-difference response depends sensitively on the retardation of the target beam, and therefore allows determining the retardation to a high degree of accuracy.

We consider a coordinate system where z is along the sample surface normal, and x and y are the in-plane coordinates. More specifically, y is in the s-polarized direction (normal to the plane of incidence), whereas both x and z contribute to the p polarization (in the plane of incidence). For achiral isotopic films (symmetry $C_{\infty\nu}$), the second-harmonic susceptibility tensor $\chi^{(2)}_{ijk}$ has the nonvanishing components ijk: zzz, $zxx = zyy$, $xxz = xzx = yyz = yzy$. The structure of the tensor implies that the p and s components of the second-harmonic field are, respectively, of the general forms [17]

$$\begin{aligned} E_p(2\omega) &= f_p E_{1p}(\omega) E_{2p}(\omega) + g_p E_{1s}(\omega) E_{2s}(\omega), \\ E_s(2\omega) &= f_s E_{1p}(\omega) E_{2s}(\omega) + g_s E_{1s}(\omega) E_{2p}(\omega), \end{aligned} \tag{2}$$

where the subscripts 1 and 2 refer to the target and probe beams, respectively. The expansion coefficients f_i and g_i are linear combinations of the components of $\chi^{(2)}_{ijk}$ and depend on the geometry of the experiment. For the two circular probe polarizations [$E_{2s}(\omega) = \pm i E_{2p}(\omega)$], the intensities of the p and s components of the second-harmonic field are then proportional to

$$\begin{aligned} |E_p(2\omega)|^2 &= [|f_p|^2 |E_{1p}|^2 + |g_p|^2 |E_{1s}|^2 \pm i(f_p^* g_p E_{1s} E_{1p}^* - f_p g_p^* E_{1s}^* E_{1p})]\,|E_{2p}|^2, \\ |E_s(2\omega)|^2 &= [|f_s|^2 |E_{1p}|^2 + |g_s|^2 |E_{1s}|^2 \pm i(f_s g_s^* E_{1s}^* E_{1p} - f_s^* g_s E_{1s} E_{1p}^*)]\,|E_{2p}|^2. \end{aligned} \tag{3}$$

In general, the expansion coefficients f_i and g_i are complex numbers. For molecules with a strong nonlinearity along a single charge transfer axis, only the component β_{333} of the hyperpolarizability tensor along this axis is sufficient to describe the nonlinearity [18]. As a consequence, the nonvanishing components of the macroscopic susceptibility $\chi^{(2)}_{ijk}$ are $zxx = zyy = xxz = xzx = yyz = yzy = zzz/r$, where r is the poling ratio [18]. All coefficients f_i and g_i then depend on the same susceptibility tensor component, and no phase shift between them should occur. For our sample, the absence of a phase shift between the expansion coefficients was verified experimentally. Equations (3) then show that the only possible source of a circular-difference response is a retardation between the polarization components of the target beam.

If the symmetry of the sample is lower than $C_{\infty\nu}$, Eqs. (2) must be modified accordingly. In the most general case, each component of the second-harmonic field is specified by a set of four expansion coefficients. However, this has no influence on the reliability of the technique. In fact, even in this general case, once phase shifts between the expansion coefficients are excluded, a circular-difference response can arise only from a phase shift between the polarization components of the target beam.

We demonstrated the potential of our technique by determining the retardation of a compound zero-order half-wave plate. The wave plate was placed in the target beam, which was initially p polarized. The fast axis of the wave plate (retardation δ) was rotated by 45° from the p direction, and the polarization components of the target beam after the wave plate can be written as [19]

$$\begin{aligned} E_{1p}(\omega) &= i\cos(\delta/2) E_{10}(\omega), \\ E_{1s}(\omega) &= \sin(\delta/2) E_{10}(\omega), \end{aligned} \tag{4}$$

where $E_{10}(\omega)$ is the field amplitude of the target beam before the wave plate.

For the two circular probe polarizations, the intensities of the p and s components of the second-harmonic field are then proportional to

$$\begin{aligned} |E_p(2\omega)|^2 &= |f_p \cos(\delta/2) \pm g_p \sin(\delta/2)|^2 |E_{2p}(\omega)|^2 |E_{10}(\omega)|^2, \\ |E_s(2\omega)|^2 &= |f_s \cos(\delta/2) \mp g_s \sin(\delta/2)|^2 |E_{2p}(\omega)|^2 |E_{10}(\omega)|^2. \end{aligned} \tag{5}$$

Equations (5) show that any retardation δ different from $m\pi$ (m integer) results in a different response to left- and right-hand circular probe polarizations, unless one of the expansion coefficients f_i and g_i in each equation vanishes. In our experiment, a nominal half-wave plate was used. A deviation of the actual wave plate retardation from $\lambda/2$ ($\delta = \pi$) introduces a small circular component in the target polarization and therefore results in a circular-difference response.

A computer simulation was used to optimize the experimental geometry by assuming the ideal poling ratio $r = 3$ for the polymer film [18]. In addition, unpolarized detection of second-harmonic radiation was assumed in order to avoid any artificial circular-difference effects due to a possible misalignment of the analyzing polarizer [20]. For small incidence angles of the probe beam, the circular-difference response is large but the absolute intensity level of the signal decreases. The chosen geometry (internal incidence angles of 24° and 4.5° for the target and probe beams, respectively) results from a trade-off between these two effects. In this geometry, the magnitude of the circular-difference response [Eq. (1)] was calculated to be about 4% for a retardation error of $\lambda/1000$ of the target half-wave plate. The assumption of a poling ratio equal to 3 was waived in the theoretical model used to describe the retardation measurements, since the actual poling ratio can differ somewhat from this value.

Our sample was a spin-coated achiral thin film of the nonlinear polymer A-095.11 (Sandoz). Poling of the sample results in $C_{\infty\nu}$ symmetry. The thickness of the sample was 250 nm and its absorption maximum occurs at 502 nm.

A beam of an infrared Nd:YAG laser (1064 nm, ~5 mJ, 10 ns pulse length, 30 Hz repetition rate) was split into two beams of nearly the same intensity. To account for the refractive index of the polymer (1.676 at 1064 nm), the target and probe beams were applied on the sample at external angles of incidence of 43° and 7.5°, respectively. For accurate polarization control, the beams were initially p polarized with respect to the sample using calcite Glan polarizers (extinction ratio ~1:250 000) [21]. The zero-order half-wave plate to be tested was placed in the target beam with the fast axis oriented at 45° with respect to the p direction. A zero-order quarter-wave plate was used to manipulate the polarization of the probe beam and to access its circular polarization states.

To determine the circular-difference response and the retardation of the target wave plate as accurately as possible, the second-harmonic signal (532 nm) was recorded continuously as the probe quarter-wave plate was rotated (Fig. 2) and fitted with a theoretical model. The quality of the fit depends on the accuracy of the expansion coefficients f_i and g_i. To avoid any problems in the uncertainty of experimental parameters needed to calculate these coefficients theoretically, we determined the coefficients experimentally for the very geometry used in the subsequent retardation measurements. In addition, sufficient polarization purity of the setup was verified using s and p linearly polarized target beams: The efficiency of second-harmonic generation was always measured to be independent of the sense of circular polarization of the probe beam, within the accuracy of the technique. A typical polarization line shape and its fit are shown in Fig. 2. The fit yields the retardation of the target wave plate with a precision higher than $\lambda/10^4$. All measurements performed were in agreement with $C_{\infty\nu}$ symmetry of the sample and showed that no phase shifts occur between the expansion coefficients.

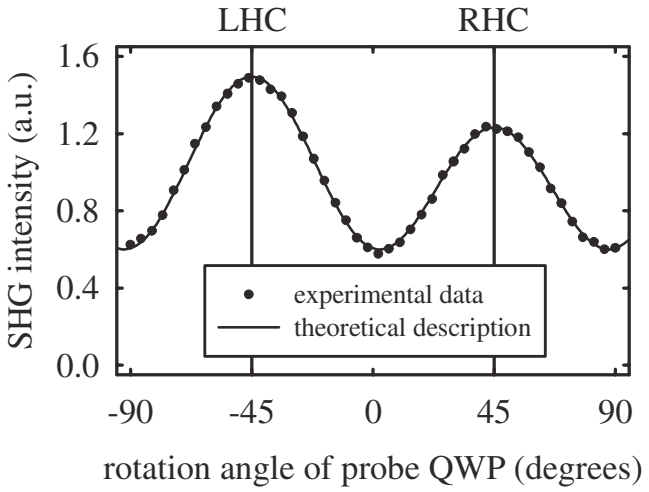

FIG. 2. Second-harmonic generation (SHG) signal as a function of the rotation angle of the probe quarter-wave plate (QWP). The angles of −45° and +45° correspond to left- (LHC) and right-hand (RHC) circularly polarized probe beams, respectively. The determined target retardation was 178.45 ± 0.03°.

The retardation of the zero-order half-wave plate was varied by tilting it about its fast axis (Fig. 3). When the difference Δn between extraordinary and ordinary refractive indices of the wave plate and the tilt angle φ are small, the retardation can be expressed as [22]

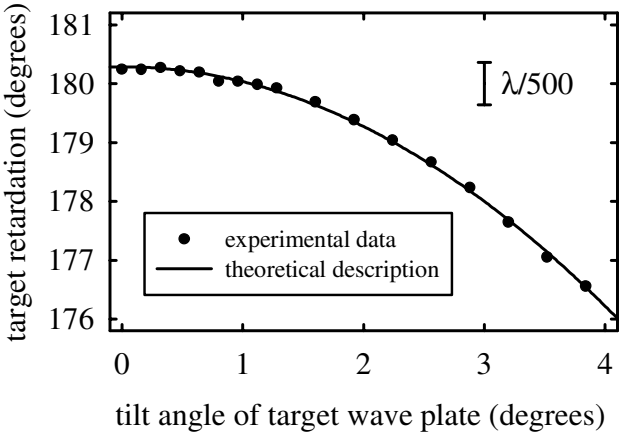

FIG. 3. Retardation of the zero-order half-wave plate as a function of its tilt angle. For comparison, a bar corresponding to a retardation of $\lambda/500$ is indicated.

$$\delta = \delta_0 - \pi \Delta n \varphi^2 d/\lambda, \quad (6)$$

where δ_0 is the retardation with the beam at normal incidence, d is the total thickness of the wave plate, and λ is the wavelength of light. The solid line in Fig. 3 is obtained by fitting the measured data to the model of Eq. (6), which yields the expected thickness ($d \cong 1$ mm) for the wave plate. The precision of each experimental retardation measurement was about $\lambda/10^4$, which is smaller than the size of the data points in Fig. 3. The deviation of some experimental points from the theoretical fit, however, is larger than this value. This is most likely due to the inhomogeneity of the wave plate [14]. If the beam is not exactly centered on the pivot point of the holder, the beam will pass through a slightly different spot on the wave plate when it is tilted. The repeatability of the technique was also measured to be at least $\lambda/10^4$.

The precision and repeatability of retardation measurements were lower when a multiorder half-wave plate was tested. This is most likely due to the high sensitivity of multiorder wave plates to temperature variations of the environment compared to zero-order wave plates [22]. For example, a temperature change on the order of 0.05 °C is sufficient to cause a retardation change of $\lambda/10^4$ in typical multiorder half-wave plates [22].

We performed a detailed analysis of the sensitivity of the technique to various sources of errors. The technique is remarkably insensitive to misalignments of the beams and of the optical components, as well as to errors in the retardation of the probe quarter-wave plate. The physical reason for this is the fact that the circular-difference response arises directly from interference between the real and imaginary parts of the polarization vectors of the fundamental beams. Misalignments of the optical components and of the fundamental beams do not introduce any additional imaginary component in their polarization states. Clearly, the quality of the wave plate used in the probe beam influences its polarization state. However, the (near) circular probe polarizations are mainly used to detect the presence of an imaginary part in the target polarization. Therefore, small deviations of the quarter-wave plate retardation from $\delta = \pi/2$ can be tolerated without significantly affecting the precision of the technique.

The values for the target retardation obtained when allowing reasonable deviations of the above parameters from the ideal values are well within the precision of the techniques. As an example, a deviation of $\lambda/1000$ from an ideal probe quarter-wave plate would lead only to an error on the order of $\lambda/40\,000$ in the determination of the target retardation for the retardation range investigated.

In the initial demonstration of the technique, we investigated the special case of a target half-wave plate (retardation $\delta = \pi$). We have also found that the extension of the technique to small values of retardation (around $\delta = 0$) is straightforward. This opens up a vast field of possible applications in the study of low-level residual birefringence in optical components [14]. We are also investigating ways to extend the technique to measure arbitrary values of retardation with the same precision.

In conclusion, we have demonstrated a highly sensitive nonlinear optical technique for retardation measurements. The technique relies on fundamental symmetry properties of nonlinear interactions and does therefore not require sophisticated experimental arrangement or data analysis to achieve a high precision. In the initial demonstration of the technique using a simple experimental setup, we already achieved a precision and repeatability better than $\lambda/10^4$. We believe that these values can be further improved by future refinements in the experimental details.

S. C. acknowledges support by the Centre for International Mobility and the Graduate School of Modern Optics and Photonics in Finland.

*Email address: stefano.cattaneo@tut.fi

[1] See, for example, S. Huard and G. Vacca, *Polarization of Light* (Wiley, New York, 1997).
[2] See, for example, J. Hecht, *Understanding Fiber Optics* (Prentice-Hall, New York, 1999).
[3] R. Holzwarth, Th. Udem, and T. W. Hänsch, Phys. Rev. Lett. **85**, 2264 (2000).
[4] M. Born and E. Wolf, *Principles of Optics* (Pergamon Press, Oxford, 1980).
[5] See, for example, A. R. Bungay, S. V. Popov, and N. I. Zheludev, Opt. Lett. **20**, 356 (1995).
[6] S. C. Read *et al.,* J. Opt. Soc. Am. B **5**, 1832 (1988).
[7] F. Brandi, E. Polacco, and G. Ruoso, Meas. Sci. Technol. **12**, 1503 (2001).
[8] J. Y. Lee *et al.,* Appl. Opt. **39**, 1941 (2000).
[9] Meadowlark Optics, Polarization Handbook, 1998–2001.
[10] L. Yao, Z. Zhiyao, and W. Runwen, Opt. Lett. **13**, 553 (1988).
[11] S. Nakadate, Appl. Opt. **29**, 242 (1990).
[12] K. B. Rochford and C. M. Wang, Appl. Opt. **36**, 6473 (1997).
[13] Y. Zhang *et al.,* Opt. Eng. **40**, 1071 (2001).
[14] B. Wang and T. C. Oakberg, Rev. Sci. Instrum. **70**, 3847 (1999).
[15] B. Wang and W. Hallman, Rev. Sci. Instrum. **72**, 4066 (2001).
[16] Y. R. Shen, *The Principles of Nonlinear Optics* (Wiley, New York, 1984).
[17] T. Verbiest, M. Kauranen, and André Persoons, Phys. Rev. Lett. **82**, 3601 (1999).
[18] Ch. Bosshard *et al., Organic Nonlinear Optical Materials* (Gordon and Breach, Basel, 1995).
[19] R. M. A. Azzam and N. M. Bashara, *Ellipsometry and Polarized Light* (North-Holland, Amsterdam, 1989), p. 488.
[20] R. Stolle, M. Loddoch, and G. Marowsky, Nonlinear Opt. **8**, 79 (1994).
[21] The technique is not sensitive to any residual depolarization of the beams. In the unpolarized component, right- and left-hand circular polarizations, which lead to opposite circular-difference effects, are equally present.
[22] P. D. Hale and G. W. Day, Appl. Opt. **27**, 5146 (1988).